Lithuanian Journal of Physics, Vol. **54**, No. 4, pp. 233–243 (2014)
© Lietuvos mokslų akademija, 2014

DYNAMICS OF FREE CARRIERS – NEUTRAL IMPURITY RELATED OPTICAL TRANSITIONS IN Be AND Si δ-DOPED GaAs/AlAs MULTIPLE QUANTUM WELLS: FRACTIONAL-DIMENSIONAL SPACE APPROACH

J. Kundrotas [a], **A. Čerškus** [a], **G. Valušis** [a], **E.H. Linfield** [b], **E. Johannessen** [c],

and A. Johannessen [c]

[a] *Semiconductor Physics Institute of Center for Physical Sciences and Technology, A. Goštauto 11, LT-01108 Vilnius, Lithuania*

[b] *School of Electronic and Electrical Engineering, University of Leeds, Leeds LS2 9JT, United Kingdom*

[c] *Buskerud and Vestfold University College, Raveien 215, 3184 Borre, Norway*

E-mail: kundrot@pfi.lt

Received 12 June 2014; revised 1 October 2014; accepted 10 December 2014

The dynamics of impurity-related optical transitions in 20 nm wide silicon and beryllium δ-doped GaAs/AlAs multiple quantum wells with various doping levels has been investigated at near liquid helium temperatures. The radiative lifetimes of the free electron-neutral acceptor and the free hole-neutral donor have been identified. The capture cross-sections of the free electrons by neutral Be acceptors were experimentally determined to $\sigma_{e\text{-Be}} = 4 \times 10^{-10}$ cm, whereas this corresponded to $\sigma_{h\text{-Si}} = 2.2 \times 10^{-8}$ cm for the free holes by neutral Si donors. The experimentally determined cross-section ratio of $\sigma_{\text{h-Si}}/\sigma_{\text{e-Be}} = 55$ is close to the estimated 2*D* value of $\sigma_{h\text{-}D}/\sigma_{e\text{-}A} = 64$ and remains lower compared to the calculated value for the 3*D* case of $\sigma_{h\text{-}D}/\sigma_{e\text{-}A} = 121$.

Keywords: quantum well, photoluminescence, lifetime, capture cross-sections

PACS: 78.55.-m, 78.67.De, 78.47.jd

1. Introduction

The design and development of electronic and optoelectronic devices requires a fundamental understanding of the doping properties of impurities in semiconductor structures. The doping in two-dimensional (2*D*) quantum wells (QW) and superlattices is of particular significance, since the carrier transport properties and impurity energy levels can be varied through the material design as well as engineering the widths of wells / barriers of the constituent materials. This opens up new avenues in the realization of compact devices in which the electronic transport, optical interactions and operational frequency can be tailored for a specific application. Examples of these are photodetectors [1], which include quantum well infrared photodetectors (QWIPs) operating at infrared [2] and terahertz frequency ranges, [3] as well as terahertz sensors employing horizontal carrier transport in multiple quantum wells (MQWs) [4].

In previously reported works [5, 6], δ-doped GaAs/AlAs MQWs were investigated by measuring the photoluminescence (PL) at various excitation intensities and temperatures. A special focus was on the study of impurity optical transitions, where the line shapes generated by the impurity related transitions were shown to be asymmetric. This spectral feature of the PL is defined mainly by the spectrum of the absorption coefficient, which is the product of the carrier distribution function. A theoretical model was constructed to explain the PL line shape for different impurity types, and it was later shown (both experimentally and theoretically) that acceptor and donor related optical transitions and PL line shapes are different due to the difference in the effective masses for holes and electrons. This effect also leads to the observed differences in the generated PL spectra: for the donor-related spectrum, the luminescence band is narrower in comparison to the acceptor-related one.

The dynamics of photo excited carriers play an important role in the optical properties of QWs, and investigations have focused on the study of the lifetime of free excitons [7–10], but limited studies exist on the lifetime of free-to-bound transitions in QWs. An important characteristic parameter of the transitions (the capture cross-section) can be derived from the lifetimes of the transitions of free carriers to impurities. This is an important parameter to investigate, since

both the performance properties and the limitations of many devices depend on the capture cross-section.

The work presented in this paper focuses on the investigation of the time-resolved PL properties of beryllium (Be) and silicon (Si) δ-doped GaAs/AlAs MQWs, which were studied at the temperature of liquid helium. The emission energy of the free electron to the neutral acceptor and the free hole to the neutral donor lies within the forbidden energy gap, which is near the emission edge.

Possible mechanisms for carrier recombination are evaluated and discussed by putting a special emphasis towards the influence of doping on the radiative lifetime of the transitions by the free electron-neutral acceptor and by the free hole-neutral donor.

2. Sample fabrication and experimental procedures

The silicon or beryllium δ-doped multiple quantum wells were grown by molecular beam epitaxy on semi-insulating GaAs substrates. The samples contained a number of wells ($N = 40$), with widths (L_W) of 20 nm and separated by a 5 nm thick AlAs barrier. Each of the QWs was δ-doped (about 2 nm width) with Si donors or Be acceptors at the center of the well. The doping level for the Si doped MQWs was 4.0×10^9 cm^{-2} and 1.0×10^{10} cm^{-2}, respectively; whereas for the Be doped MQWs it was 5.0×10^{10} cm^{-2} and 2.5×10^{12} cm^{-2}, respectively.

The continuous wave (CW) PL was measured by a fully automated Horiba Jobin Yvon monochromator FHR-1000 with a focal length of 1000 mm. The spectra were dispersed with a blazed 1200 g/mm grating, and the spectral dispersion was 0.8 nm/mm. The spectral resolution of the wavelength was 0.008 nm at an exit slit width of 10 μm, and the corresponding spectral resolution of the energy was 0.015 meV at 820 nm. An Ar-ion laser was used as the excitation source with excitation energy in the range of 2.2–2.7 eV. The PL was detected by a thermoelectrically cooled Hamamatsu GaAs photomultiplier operating in the photon counting regime. The photon emission was measured using a Becker & Hickl gated photon counter/multiscaler [11].

The time-resolved PL measurements were performed using a Standa Company's frequency-doubled diode-pumped Nd:LSB microchip solid-state laser with 400 ps FWHM pulse width. The pulse repetition rate was 10 kHz, while the average output power was set to 40 mW. The excitation wavelength was 531 nm (photon energy of 2.3 eV). The transient PL was measured using a Becker & Hickl time correlated single photon counting (TCSPC) system [12]. The emitted photons were detected with a thermoelectrically cooled, high efficiency, extended-red, multi-alkali cathode photomultiplier with an internal GHz preamplifier. To avoid the jitter effect, the measured signal was synchronized with a laser pulse from a split excited beam. The excitation intensity was varied by using neutral glass filters.

The sample temperatures were changed from ambient room temperature (300 K) down to 3.6 K using a closed cycle helium optical cryostat (Janis Research Company 1 W @4.2 K model SHI-4). The cryostat was equipped with two thermometers: the first one was used to control the operation of the equipment and the second one was used to measure the temperature of the sample.

The CW PL spectrum was compared to the spectrum obtained using a picoseconds laser by implementing two different methods. The first method (direct electronically integrated method) registers photons with a GaAs photomultiplier attached to a direct electronic integration gated photon counter/multiscaler, which was the same as in the original CW PL method. In the second method (TCSPC integrated method) a computer code was used to process the results obtained from the TCSPC measurements.

3. Experimental results

The CW PL spectra of the Be d-doped GaAs/AlAs sample for $L_W = 20$ nm ($N_{\mathrm{Be}} = 5.0 \times 10^{10}$ cm^{-2}) MQWs measured at a temperature of 3.6 K and at a laser excitation intensity of $I = 1.36$ W/cm^2 are shown in Fig. 1. A series of clearly resolved peaks can be seen. The most intensive PL band is associated with the excitons bound to the acceptor impurities, and is labeled as [BeX]. It is also possible to discriminate the line originating from the heavy-hole excitons labeled as $X_{e1\text{-}hh1}$. The lower energy transitions, labeled as e-Be, are attributed to the recombination of the free electrons with holes bound to a neutral Be acceptor.

The CW PL spectrum was also compared to the measured spectra obtained using picosecond laser excitation (Fig. 1). The PL spectrum was measured at a pulse excitation of $I_{\mathrm{imp}} = 70$ W/cm^2 which would be equivalent to an average excitation intensity of $I_{\mathrm{av}} = 0.28$ mW/cm^2. Two methods were used to record the measurements. The upper line curve shown in Fig. 1 is obtained using a direct electronically integrated method, whereas the dot curve represents the plot for e-Be band emission obtained using the TCSPC integrated method. It can be seen that the character of the spectrum for all the measured cases is the same. However, the relative intensity of the lines is dependent on the laser excitation intensity. The lines related to the impurity PL emission reach saturation because

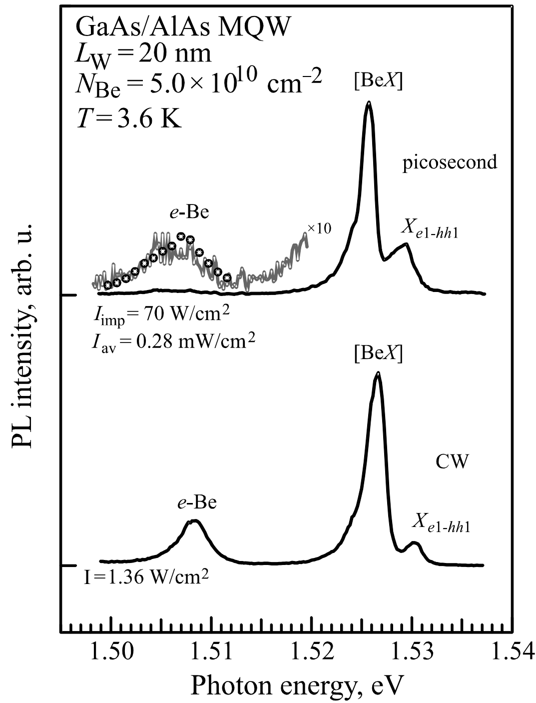

Fig. 1. The PL spectra of the Be δ-doped GaAs/AlAs sample for L_W = 20 nm (N_{Be} = 5.0 × 10^{10} cm^{-2}) MQWs recorded at a temperature of 3.6 K. The laser excitation intensity was I = 1.36 W/cm^2 for the CW measured method and I_{imp} = 70 W/cm^2 or I_{av} = 0.28 mW/cm^2 for the two measured methods with pulse excitation. The line plot and dots correspond to a direct electronical integration and TCSPC integration respectively. The symbols: $X_{e1\text{-}hh1}$ is the heavy-hole exciton, [BeX] is the Be acceptor-bound exciton, and e-Be is the free electron-neutral Be acceptor transitions. The curves are shifted vertically for clarity.

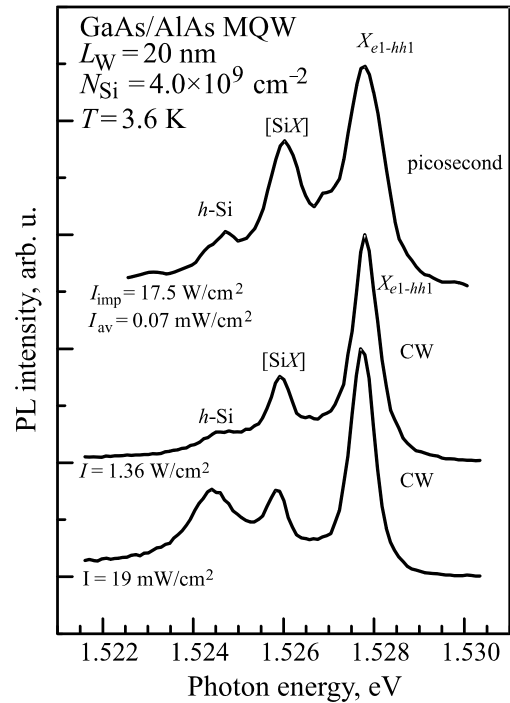

Fig. 2. The PL spectra of the Si δ-doped GaAs/AlAs samples for L_W = 20 nm (N_{Si} = 4.0 × 10^9 cm^{-2}) MQWs recorded at 3.6 K. The laser excitation intensity of I = 19 mW/cm^2 or I = 1.36 W/cm^2 for CW measured method, and I_{imp} = 17.5 W/cm^2 or I_{av} = 0.07 mW/cm^2 for measurements using the direct electronically integrated method. The symbols: $X_{e1\text{-}hh1}$ is the heavy-hole exciton, [SiX] is the Si donor-bound exciton, and h-Si is the free hole-neutral Si donor transitions. The spectra are shifted vertically for clarity.

of the impurity concentration being finite. Also one should note that the excitonic lines may merge into one band and the spectrum from the fine structures might disappear. In order to exclude these effects we measured the PL spectrum at a pulse excitation. In Fig. 1 we observe a small shift between the spectra of CW and the pulse excitation. It is related to the different excitation intensities as previously presented in a previous publication [6]. From the obtained results it was concluded that the peak excitation intensity of the pulsed laser (instead of the average excitation intensity) was the most correct parameter to use when interpreting factors that influenced the structure of the spectrum.

The CW PL spectra of the donor Si δ-doped GaAs/AlAs samples for L_W = 20 nm (N_{Si} = 4.0 × 10^9 cm^{-2}) MQWs, that were measured at a temperature of 3.6 K with two laser excitation intensities of I = 19 mW/cm^2 and I = 1.36 W/cm^2, are shown in Fig. 2.

The lower energy transitions, labeled as h-Si, are attributed to the recombination of free holes with electrons which are bound to a neutral Si donor, whereas the line labeled as [SiX] is ascribed to excitons bound to Si donor impurity. The excitonic lines dominate in the silicon doped QWs with their strength being weakly related to the doping concentration. In contrast, the excitonic line strength generated by QWs doped with a Be acceptor is strongly dependent on the acceptor doping concentration [6]. The experimental results show that the structure of the PL spectrum does not change for pulse excitations up to I_{imp} = 70 W/cm^2 for the Be and Si δ-doped GaAs/AlAs MQWs.

The PL decay transients for different emission bands for the Be δ-doped sample with the lowest (N_{Be} = 5.0 × 10^{10} cm^{-2}) at T = 3.6 K and at a laser excitation intensity of I_{imp} = 70 W/cm^2 are shown in Fig. 3. The average power excitation intensity was estimated to 0.28 mW/cm^2.

The transition lifetimes of the free electron to the acceptor in p-type MQWs and the free hole to the donor

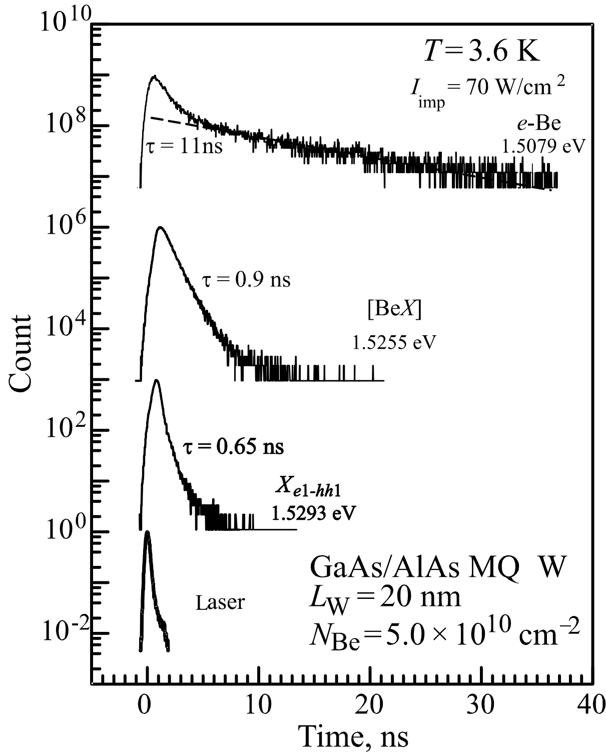

Fig. 3. The PL decay transients of different emission bands for the lowest Be δ-doped sample (N_{Be} = 5.0 × 10^{10} cm^{-2}) recorded at T = 3.6 K and at a laser excitation intensity of I_{imp} = 70 W/cm^2. The lowest curve indicates the response of the laser excitation pulse. The decay time constants and emission energies are marked for each trace. The curves are offset vertically for clarity. The abbreviations are the same as in Fig. 1.

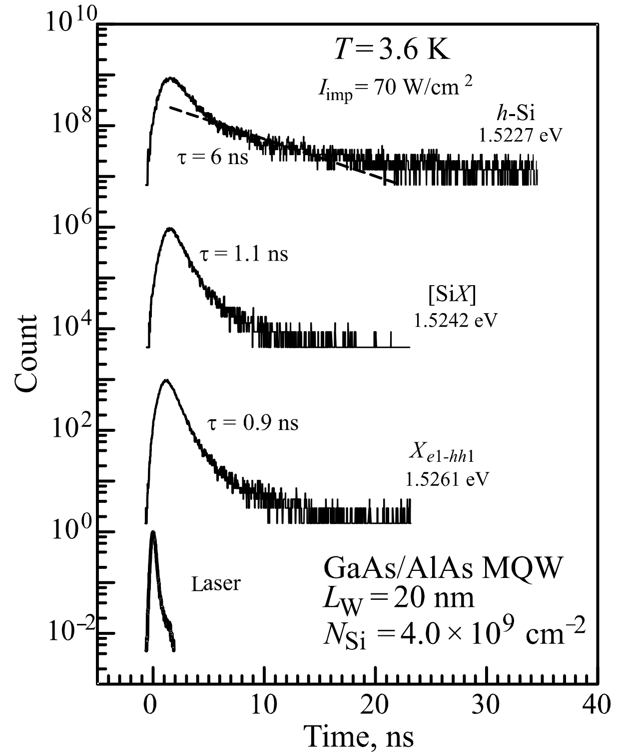

Fig. 4. The PL decay transients of different emission bands for the lowest Si δ-doped sample (N_{Si} = 4.0 × 10^9 cm^{-2}) at T = 3.6 K and a laser excitation intensity of I_{imp} = 70 W/cm^2. The lowest curve indicates the response of the laser excitation pulse. The decay time constants and emission energies are indicated on each trace. The curves are offset vertically for clarity. The abbreviations relate to Fig. 2.

in n-type MQWs were extracted from the data when fast excitonic processes were quenched. The free exciton emission decay was estimated to be around $\tau_{X_{e1-hh1}}$ = 0.65 ns, whereas the bound exciton emission decay time was found to be equal to $\tau_{[BeX]}$ = 0.9 ns. The values of the excitonic emission decay times are consistent with the previously obtained data reported in literature [7–10]. These are dependent on the factors such as the quantum well width and homogeneity, as well as doping type and impurity concentrations.

The transition decay time of the free electron Be acceptor was estimated to $\tau_{e\text{-Be}}$ = 11 ns. This is in good agreement with that previously reported for 15 nm MQWs [13] as well as the results published in [14] at low temperatures ($\tau_{e\text{-Be}}$ = 34 ns) and at a doping concentration of N_{Be} = 10^{10} cm^{-2}. For the 2.5 × 10^{12} cm^{-2} Be doped sample, the lifetime was too short to be measured and was estimated to be in the order of a few hundred ps.

Figure 4 shows the PL decay transients for different emission bands for the lowest Si δ-doped sample (N_{Si} = 4.0 × 10^9 cm^{-2}) at T = 3.6 K and at a laser excitation intensity of I_{imp} = 70 W/cm^2.

The free exciton emission decay constant was $\tau_{X_{e1-hh1}}$ = 0.9 ns, the bound exciton emission decay time was found to be $\tau_{[SiX]}$ = 1.1 ns, whereas the free hole-Si donor transition decay time was estimated to be $\tau_{h\text{-Si}}$ = 6 ns.

A comparison of the PL decay transients of the free hole-neutral Si donor transitions for two Si δ-doped samples: N_{Si} = 4.0 × 10^9 cm^{-2} and N_{Si} = 1.0 × 10^{10} cm^{-2} at T = 3.6 K are shown in Fig. 5.

The recombination lifetime for the sample with N_{Si} = 4.0 × 10^9 cm^{-2} is equal to $\tau_{h\text{-Si}}$ = 6 ns whereas for a Si concentration of N_{Si} = 1.0 × 10^{10} cm^{-2} it was equal to $\tau_{h\text{-Si}}$ = 2.6 ns. These results show that the lifetime is inversely proportional to the impurity concentration not only for the free electron to acceptor transitions [13] but also for the free hole to donor transitions, i. e. $\tau_{e\text{-}A}$~$1/N_A$ and $\tau_{h\text{-}D}$~$1/N_D$. However, as we have shown in a previous publication [13], this relation is not valid for transitions close to Mott's or above where the impurity bands or two dimensional

electron gases are formed due to high doping concentrations.

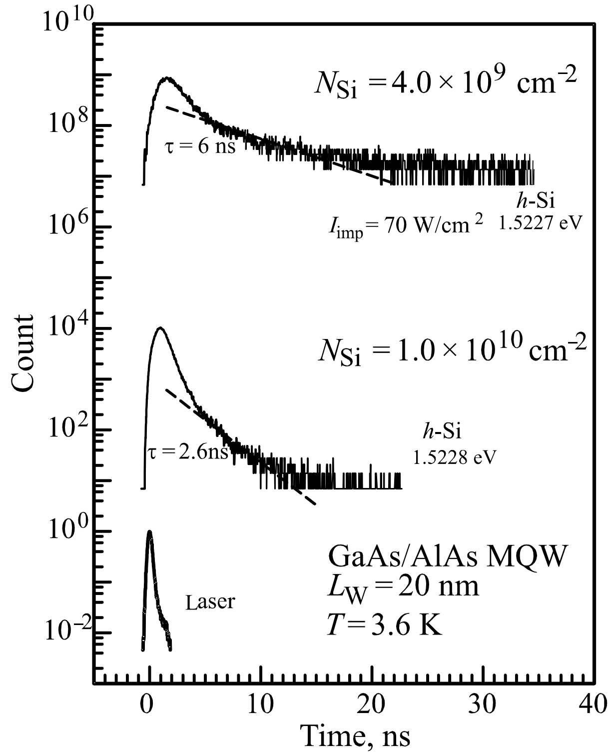

Fig. 5. The PL decay transients of the free hole-neutral Si donor transitions for two Si δ-doped samples ($N_{Si} = 4.0 \times 10^9$ cm^{-2} and $N_{Si} = 1.0 \times 10^{10}$ cm^{-2}) at $T = 3.6$ K and a laser excitation intensity of I_{imp} = 70 W/cm^2. The lowest curve indicates the response of the laser excitation pulse. The decay time constants and emission energies are marked on each trace. The curves are offset vertically for clarity.

4. Analysis of experimental results

A fundamental understanding of the impurity effects is required to predict the electronic, optical and carrier transport properties of doped QWs. For the *e*-A transitions, the capture of the free hole after electron recombination with the neutral acceptor is of particular importance. Experiments show that the hole trapping time using an ionizing acceptor is much faster compared to the *e*-A transition with an estimated value of around τ_{h-A^-} = 5 ps [15]. Hence, this measured lifetime corresponds to the lifetime of the free electron to acceptor transition and thus we can calculate the capture cross-section for this particular process.

The capture cross-section of the free electron-acceptor radiative recombination can be expressed by the phenomenological relation:

$$\sigma_{e-A} = \frac{1}{\tau_{e-A} N_A v_{e,th}}, \qquad (1)$$

where τ_{e-A} is the radiative recombination lifetime, N_A is the acceptor concentration, and $v_{e,th}$ is the average thermal velocity of the electrons which is equal to

$$v_{e,th} = \sqrt{\frac{8kT}{\pi m_c^*}}\,. \qquad (2)$$

For two dimensional structures, the impurity concentration N_A is measured in units of cm^{-2} whereas the units of the capture cross-section σ_{e-A} are in cm.

Using the effective mass of the electron m_c^* = 0.0665 m_0 [16] the thermal velocity of electrons, which is estimated at a temperature of T = 3.6 K, is equal to $v_{e,th} = 4.6 \times 10^6$ cm/s. Consequently, the measured recombination lifetime for the Be δ-doped $N_{Be} = 5.0 \times 10^{10}$ cm^{-2} MQWs is equal to τ_{e-Be} = 11 ns, whereas the capture cross-section will be equal to $\sigma_{e-Be} \approx 4.0 \times 10^{-10}$ cm.

A similar situation occurs for the *h-D* transition processes. Although the recombination speed is unknown, it is important to understand how the capture of free electrons occurs after the holes recombine with neutral donors. The results suggest that the electron trapping coefficient by an ionizing donor is equal to B_D = 1 cm^2/s [17]. Normally, Si in GaAs can be considered as an amphoteric impurity, which exhibits predominantly donor characteristics when embedded in GaAs grown by molecular beam epitaxy. However, depending on the GaAs growth conditions, there will always be a small part of Si atoms (8–20%) which become acceptors [18, 19]. Using the relation $\tau_{e-D^+} = 1/(B_D N_D^+)$ the trapping time can be estimated to around 1 ns for the lower doped sample and around 0.5 ns for the higher doped Si sample. Therefore, the measured impurity-related lifetime in Si doped quantum wells can be attributed to the transitions of the free holes to donor impurities with a negligible error.

The capture cross-section of the free hole-donor radiative recombination can be calculated by adapting expressions (1) and (2) replacing the acceptor concentration with the donor concentration and the effective mass of the electrons with the effective mass of the holes. Using the effective mass of holes m_p^* = 0.38 m_0 [6, 20] at T = 3.6 K, the thermal velocity of holes would be equal to $v_{h,th} = 1.92 \times 10^6$ cm/s. Consequently, for the Si δ-doped $N_{Si} = 4.0 \times 10^9$ cm^{-2} MQWs, the measured recombination lifetime is equal to $\tau_{h\text{-}Si}$ = 6 ns which corresponds to a capture cross-section of $\sigma_{h\text{-}Si} \approx 2.2 \times 10^{-8}$ cm. For the sample with a Si concentration of $N_{Si} = 1.0 \times 10^{10}$ cm^{-2}, the recombination

lifetime is $\tau_{h\text{-Si}}$ = 2.6 ns which leads to a capture cross-section of $\sigma_{h\text{-Si}} \approx 2.0 \times 10^{-8}$ cm, which coincides well with the other sample result.

5. Theoretical analysis and discussion

A theoretical analysis of the impurity related recombination processes in quantum wells will be based on quantum mechanics in the fractional dimensional space FDS) [21]. In previously reported papers, the FDS approach was used to calculate the optical properties of impurity-related CW PL [5, 6], as well as estimating the Huang-Rhys factor in multiple quantum wells [22].

The free electon-acceptor radiative recombination lifetime and the free hole-donor radiative recombination lifetime will be considered first. Then, the ratio of the capture cross-sections of the free hole-donor radiative recombination and the free electron-acceptor radiative recombination ($\sigma_{h\text{-}D}/\sigma_{e\text{-}A}$) will be compared to the experimental results.

It is well known that low-dimensional systems are highly anisotropic, and experimental data obtained, for instance in semiconductor QWs, can be analyzed using isotropic coordinate systems possessing anisotropic Hamiltonians. In the idealized case for infinite QWs, the system is presumed to be exactly two-dimensional (2*D*). However, in real structures (not infinite QWs) excitons or impurities are not 2*D* anymore. They are in a medium intermediate between 2*D* and 3*D* systems since the electron- or hole-wave function penetrates the barrier in the confining dimension. We can therefore consider the structures in another manner, i. e. by applying the FDS approach [21] and assuming that an anisotropic system in 3*D* space can be treated as isotropic or unconfined in the effective FDS [23, 24]. In this case the single parameter – dimensionality – contains all the information about the anisotropy or confinement of the low dimensional system.

Shallow impurities can be considered as hydrogen-like atoms, and hence the FDS approach can be extended to describe these systems. In that case the discrete bound-state energies and orbital radii for excitons and impurities, i. e. a hydrogen-like system, can be given as follows [25]:

$$E_n = \frac{Ry}{\left[n + \frac{\alpha - 3}{2}\right]^2}, \tag{3}$$

$$a_n = a_0\left[n + \frac{\alpha - 3}{2}\right]^2, \tag{4}$$

where $n = 1, 2, \ldots$ is the principal quantum number, *Ry* and a_0 denote the Rydberg energy and Bohr radius for the exciton or hydrogen-like impurity in the three-dimensional (3*D*) case, and α labels the dimensionality parameter which changes from 2 to 3 for idealized QWs. For the 2*D* case, when $\alpha = 2$, the binding energy of the 1s exciton or impurity is a factor of four greater than for the 3*D* case, i. e. $E_1 = 4Ry$.

The impurity binding energy in αD space from Eq. 1 for $n = 1$ is equal:

$$E_I = Ry_I\left(\frac{2}{\alpha - 1}\right)^2. \tag{5}$$

We adapt the Dumke's [26] model and use the fractional dimensional space approach [5].

The total spontaneous emission rate is obtained by summing over all radiation modes [26, 27] and is equal to

$$R_{sp} = \int R_{sp}(\hbar\omega)\mathrm{d}\hbar\omega = \int P_{(c,v)\,k,\,(D,A)}\, D_\alpha(\hbar\omega)\mathrm{d}(\hbar\omega). \tag{6}$$

The index *c* means the conduction band, *v* means the valence band, *D* is a donor, *A* is an acceptor, respectively. $P_{(c,v)k,(D,A)}$ is the optical transition probability between the conduction band state and an acceptor level or between the valence band state and a donor induced by the interaction of one electromagnetic mode. $D_\alpha(\hbar\omega)$ is the photon density of states which is a current case in the fractional dimensional space. Considering the free electron acceptor *e-A* transitions, the transition probability $P_{c,k,A}$ in FDS can be described by [5]

$$P_{ck,A} = \frac{4\pi^2 e^2}{n_B c m_0^2 \omega}|d_{cv}|^2 |a(k)|^2 \times \delta(\hbar\omega - E_{QW} - E_{ck} + E_A), \tag{7}$$

where $|d_{cv}|^2$ is the conduction-to-valence squared matrix element of the electron dipole moment, $a(\mathbf{k})$ is the Fourier transformation of an impurity hydrogen-like function, and E_{QW} is the forbidden energy gap. Considering the 3*D* case, $E_{QW} = E_g$, whereas for the 2*D* case this is the energy between the heavy hole E_{hh1} and the electron E_{e1} energy levels in QW's.

For a hydrogen-like approximation of the acceptor impurity and simple valence band structure, shallow acceptor wave functions can be expanded as a linear combination of valence band functions and the motion of free carriers. These can be described by a plane wave function in the FDS [21], and leads to the result that a(k) is the Fourier transformation of the acceptor hydrogen-like function [28]:

$$a(k) = \int \mathrm{e}^{-i\mathbf{kr}} F(\mathbf{r})\mathrm{d}r, \tag{8}$$

where $F(\mathbf{r})$ is the acceptor hydrogen-like function in FDS [25]:

$$F(r) = \left[\frac{2^{\alpha+1} \pi^{\frac{1-\alpha}{2}}}{\Gamma\left(\frac{\alpha-1}{2}\right)(\alpha-1)^{\alpha+1}} \frac{1}{a_B^{\alpha}} \right]^{1/2} e^{-\frac{2}{\alpha-1}\frac{r}{a_B}}, \quad (9)$$

where a_B is the acceptor Bohr radius in the 3D case. The Fourier transformation in FDS reads as follows [21]:

$$a(k) = (2\pi)^{\alpha/2} \int_0^{\infty} r^{\alpha-1} (kr)^{1-\frac{\alpha}{2}} \mathrm{J}_{\frac{\alpha}{2}-1}(kr) F(r) \mathrm{d}r, \quad (10)$$

where $\mathrm{J}_{\frac{\alpha}{2}-1}(kr)$ represents the Bessel function. The coefficient squared $|a(\mathbf{k})|^2$ in FDS is given by

$$|a(k)|^2 = 2^{\alpha} \pi^{\frac{\alpha-1}{2}} (\alpha-1)^{\alpha} \Gamma\left(\frac{1+\alpha}{2}\right) \times \frac{a_B^{\alpha}}{V_{\alpha}\left[1 + a_B^2 k^2 \left(\frac{\alpha-1}{2}\right)^2\right]^{1+\alpha}}. \quad (11)$$

Using the parabolic relation of E and k, $E = (\hbar^2 k^2)/(2m^*)$, the energy dependence of the coefficient squared $|a(\mathbf{k})|^2$ of the e-A transitions in the FDS space is given by

$$|a(k)|^2 = \frac{2^{\alpha/2} \pi^{\frac{\alpha-1}{2}} (\alpha-1)^{\alpha} \Gamma\left(\frac{1+\alpha}{2}\right)}{\left(m_p^* Ry_A\right)^{\alpha/2}} \times \frac{1}{\left[1 + \left(\frac{m_c^*}{m_p^*}\right) \frac{E}{Ry_A \left(\frac{2}{\alpha-1}\right)^2}\right]^{1+\alpha}}. \quad (12)$$

where m_c^* is the effective mass of the conduction band carriers, m_p^* is the effective mass of holes, and Ry_A is the acceptor impurity binding energy in the 3D case. Consequently, we can similarly write the coefficient squared $|a(\mathbf{k})|^2$ of h-D transition.

At $\mathbf{k} = 0$, the highest transition probability $|a(\mathbf{k})|^2$ is equal to

$$|a(\mathbf{k}=0)|^2 = \frac{2^{\alpha/2} \pi^{\frac{\alpha-1}{2}} (\alpha-1)^{\alpha} \Gamma\left(\frac{1+\alpha}{2}\right)}{\left(m_p^* Ry_A\right)^{\alpha/2}}. \quad (13)$$

After inserting (12) into (7), the transition probability $P_{ck,A}$ in the FDS space is equal to

$$P_{ck,A} = \frac{2^{\alpha/2+2} \pi^{(\alpha+3)/2} e^2 (\alpha-1)^{\alpha} \Gamma\left(\frac{1+\alpha}{2}\right) \hbar^{\alpha+1}}{n_B^2 m_0^2 \hbar\omega \left(m_p^* Ry_A\right)^{\alpha/2} L^{3-\alpha}} \times \frac{|d_{cv}|^2 \delta(\hbar\omega - E_{QW} - E_{ck} + E_A)}{\left[1 + \left(\frac{m_c^*}{m_p^*}\right) \frac{E}{Ry_A \left(\frac{2}{\alpha-1}\right)^2}\right]^{1+\alpha}}. \quad (14)$$

For the 3D case, this exactly coincides with the Dumke's [26] theory equation (6). Adopting the SI system requires a change of e^2 to $e^2/(4\pi\varepsilon_0)$. For the 2D case the transition probability can be written as

$$P_{ck,A} = \frac{4\pi^3 e^2 \hbar^3}{n_B^2 m_0^2 \hbar\omega \left(m_p^* Ry_A\right) L} \times \frac{|d_{cv}|^2 \delta(\hbar\omega - E_{QW} - E_{ck} + E_A)}{\left[1 + \left(\frac{m_c^*}{m_p^*}\right) \frac{E}{4 Ry_A}\right]^{3}}. \quad (15)$$

Consequently, similar formulas can be written for the h-D transitions. The density of electromagnetic modes $D_{\alpha}(\hbar\omega)$ [29] using [23] ideology in FDS can be expressed as

$$D_{\alpha}(E)\mathrm{d}E = \frac{2}{(2\pi)^{\alpha}} \mathrm{d}^{\alpha} k_v, \quad (16)$$

where the photon energy is equal to $E = \hbar\omega$. Factor 2 includes two polarizations [29] where the $\mathrm{d}^{\alpha} k_v$ is equal to

$$\mathrm{d}^{\alpha} k_v = \frac{2\pi^{\alpha/2}}{\Gamma(\alpha/2)} k_v^{\alpha-1} \mathrm{d}k_v. \quad (17)$$

Using $k_v = E/(\hbar c) = \omega/c$, we get $\mathrm{d}k_v/\mathrm{d}E = 1/(\hbar c)$ and the term $D_{\alpha}(\hbar\omega)$ in vacuum can be expressed as

$$D_{\alpha}(\hbar\omega) = \frac{2}{(2\pi)^{\alpha}} \frac{2\pi^{\alpha/2}}{\Gamma(\alpha/2)} \frac{1}{\hbar c^{\alpha}} \omega^{\alpha-1}. \quad (18)$$

Considering a medium with refractive index n_B, the light speed in vacuum will be changed to the speed in the medium c/n_B, which makes $D_{\alpha}(\hbar\omega)$ equal to

$$D_{\alpha}(\hbar\omega) = \frac{2}{(2\pi)^{\alpha}} \frac{2\pi^{\alpha/2}}{\Gamma(\alpha/2)} \frac{n_B^{\alpha}}{\hbar c^{\alpha}} \omega^{\alpha-1}. \quad (19)$$

The recombination rate is given as

$$\frac{n}{\tau_{e-A}} = N_A \int_0^\infty R_{ck,A} f_c(E_c) G_\alpha(E_c) \mathrm{d}E_c\,, \tag{20}$$

where N_A is the concentration of acceptors in the $3D$ case [1/cm^3] and in the $2D$ case [1/cm^2]. $\tau_{e\text{-}A}$ is the electron lifetime for the free electron to neutral acceptor transition, and $f_c(E_c)$ is the occupation probability of electrons in the conduction band [30], which can be described by

$$f_c(E_c) = \frac{n\mathrm{e}^{-E_c/(kT)}}{2\left(\frac{m_c^* kT}{2\pi\hbar^2}\right)^{\alpha/2}}\,. \tag{21}$$

The denominator is the effective density of states in the conduction band $N_c = 2\left[m_c^* kT/(2\pi\hbar^2)\right]^{\alpha/2}$ written in FDS. The term $G_\alpha(E_c)$ in (20) represents the density of states in the FDS approach and is expressed as follows [23]:

$$G_\alpha(E_c) = \frac{2}{\Gamma\left(\frac{\alpha}{2}\right)}\left(\frac{m_c^*}{2\pi\hbar^2}\right)^{\alpha/2} E_c^{\alpha/2-1}, \tag{22}$$

where factor 2 takes into account the spin degeneracy.

The inverse lifetime of the electron recombination with the bound hole on the acceptor is equal to

$$\frac{1}{\tau_{e-A}} = \frac{2^{4-\alpha/2}\pi^{3/2} n_B^{\alpha-2} e^2 (\alpha-1)^\alpha \Gamma\left(\frac{1+\alpha}{2}\right)\hbar(\hbar\omega)^{\alpha-2}|d_{cv}|^2}{\Gamma\left(\frac{\alpha}{2}\right) c^\alpha m_0^2 \left(m_p^* Ry_A\right)^{\alpha/2} L^{3-\alpha}} \times \gamma_{e-A}(T)\, N_A. \tag{23}$$

Consequently, the inverse lifetime of hole recombination with the bound electron on the donor is equal t

$$\frac{1}{\tau_{h-D}} = \frac{2^{4-\alpha/2}\pi^{3/2} n_B^{\alpha-2} e^2 (\alpha-1)^\alpha \Gamma\left(\frac{1+\alpha}{2}\right)\hbar(\hbar\omega)^{\alpha-2}|d_{cv}|^2}{\Gamma\left(\frac{\alpha}{2}\right) c^\alpha m_0^2 \left(m_c^* Ry_D\right)^{\alpha/2} L^{3-\alpha}} \times \gamma_{h-D}(T)\, N_D, \tag{24}$$

where $L^{3-\alpha}$ is a scaling parameter or the distance of medium. In the case MQWs L is a periodic function of $L = L_W + L_B$ [31], Equations (23) and (24) for the $3D$ case at **k** = 0 are identical for Dumke's [26] formulas (15) and (14).

Considering the $2D$ case

$$\frac{1}{\tau_{e-A}} = \frac{4\pi^2 e^2 \hbar |d_{cv}|^2}{c^2 m_0^2 (m_p^* Ry_A)\, L}\gamma_{e-A}(T) N_A, \tag{25}$$

$$\frac{1}{\tau_{h-D}} = \frac{4\pi^2 e^2 \hbar |d_{cv}|^2}{c^2 m_0^2 (m_p^* Ry_D)\, L}\gamma_{h-D}(T) N_D\,. \tag{26}$$

When **k** = 0, the parameters $\gamma_{e\text{-}A}$ and $\gamma_{h\text{-}D}$ are equal units both in the $2D$ and $3D$ cases.

The conduction-to-valence squared matrix element of the electron dipole moment $|d_{cv}|^2$ is related to the Kane parameter, which for GaAs is equal to E_p = 22.71 eV [32]. Hovewer, $|d_{cv}|^2$ is different in the $3D$ and the $2D$ cases. Considering the $3D$ case in GaAs, both the *hh* and *lh* states are degenerate and include transition selection rules [33] which leads to $|d_{cv}|^2 = m_0E_p/12$, which are important light hole–conduction band transitions. In QW's, both the *hh* and *lh* states are no longer degenerate and constitute an important heavy hole–conduction band transition which leads to $|d_{cv}|^2 = m_0E_p/4$.

Considering the *e-A* process, the parameter $\gamma(T)$, which is a measure of the dependence of transitions probability on photon energy, equals to

$$\gamma_{e-A}(T) = \frac{1}{\Gamma(\alpha/2)(kT)^{\alpha/2}} \int_0^\infty \frac{\mathrm{e}^{-E_c(kT)} E_c^{\alpha/2-1}\mathrm{d}E_c}{\left[1 + \frac{m_c^*}{m_p^*}\frac{E_c}{Ry_A\left(\frac{2}{\alpha-1}\right)^2}\right]^{\alpha+1}}\,, \tag{27}$$

where k is the Boltzmann constant. Using $y = m_c^*E/(m_c^*Ry_A)$ and $\beta = m_p^*\, Ry_A/(m_c^*kT)$, the combination yields the following:

$$\gamma(\beta) = \frac{1}{\Gamma(\alpha/2)}\beta^{\alpha/2}\int_0^\infty \frac{\mathrm{e}^{-\beta y} y^{\alpha/2-1}\,\mathrm{d}y}{\left[1 + y\left(\frac{\alpha-1}{2}\right)^2\right]^{\alpha+1}}. \tag{28}$$

Considering the *h-D* process, $y = m_p^*E/((m_c^*Ry_D)$ and $\beta = m_c^*Ry_D/(m_p^*kT)$.

The cross-section ratio of $\sigma_{h\text{-Si}}/\sigma_{e\text{-Be}}$ is a good parameter to compare experimental and theoretical results because this process requires only a few parameters of materials to be considered. Using (1), (23) and (24) the cross-section ratio is equal to

$$\frac{\sigma_{h-D}}{\sigma_{e-A}} = \frac{\gamma_{h-D}}{\left(m_c^* Ry_D\right)^{\alpha/2} v_{h,th}} \frac{\left(m_p^* Ry_A\right)^{\alpha/2} v_{e,th}}{\gamma_{e-A}}. \quad (29)$$

Considering that the impurity Ry energy is proportional to the effective mass $Ry \sim m^*$ and the thermal velocity is proportional to the square root of the inverse mass of the carrier $v_{th} \sim 1/\sqrt{m^*}$, then Eq. (29) may be overwritten as follows:

$$\frac{\sigma_{h-D}}{\sigma_{e-A}} = \left(\frac{m_p^*}{m_c^*}\right)^{\alpha+1/2} \frac{\gamma_{h-D}}{\gamma_{e-A}}, \quad (30)$$

where $\alpha = 3$ (in the $3D$ case) and $\alpha = 2$ (in the $2D$ case), whereas γ_{e-A} and γ_{h-D} are the parameters (28) for the e-A and h-D transitions, respectively. For the wave vector $\mathbf{k} = 0$, the transition lifetime is the shortest whereas the recombination probability is at a maximum. The transition lifetime for the carriers with higher energies will be increased due to smaller transition probability. The parameters γ_{e-A} and γ_{h-D} are in the order of unity for the $2D$ case.

The theoretical expressions will be used to calculate numerical data for comparison with the experimental results. All numerical calculations are performed at a temperature of $T = 3.6$ K, using a silicon impurity binding energy in the $3D$ case of 5.76 meV, a beryllium impurity in the $3D$ case of 28 meV [6] and the effective masses from Section 4. The ratio $\sigma_{h-D}/\sigma_{e-A}$, that is estimated according to (30) without corrections of γ, is equal to $\sigma_{h-D}/\sigma_{e-A} = 446$ in the $3D$ case and $\sigma_{h-D}/\sigma_{e-A} = 78$ in the $2D$ case. The parameters of γ according to (28) for the $3D$ case are equal to $\gamma_{h-D} = 0.34$ and $\gamma_{e-A} = 0.99$, respectively, and by using them we can calculate the ratio to $\sigma_{h-D}/\sigma_{e-A} = 153$. One should note that for the h-D transitions in GaAs, there is an important light hole band [26]. Including this light hole band into the calculations in the same manner as in [26] leads to a parameter of $\gamma_{h-D} = 0.27$, and the ratio of the cross-sections in the $3D$ case would now be equal to $\sigma_{h-D}/\sigma_{e-A} = 121$.

The parameters γ according to (28) for the $2D$ case are equal to $\gamma_{h-D} = 0.82$ and $\gamma_{e-A} = 1$, respectively. By applying these values, the calculated ratio according to (30) is $\sigma_{h-D}/\sigma_{e-A} = 64$, whereas the experimentally determined value (using results of Section 4) corresponds to $\sigma_{h-D}/\sigma_{e-A} = 55$.

The measured recombination lifetime for the Be δ-doped $N_{\mathrm{Be}} = 5.0 \times 10^{10}$ cm^{-2} MQWs is $\tau_{e\text{-Be}} = 11$ ns, whereas the calculated value is equal to $\tau_{e\text{-Be}} = 7.3$ ns at 3.6 K according to Eqs. (23) and (28). Consequently, for the Si δ-doped $N_{\mathrm{Si}} = 4.0 \times 10^9$ cm^{-2} MQWs, the measured recombination lifetime is $\tau_{h\text{-Si}} = 6$ ns, whereas the calculated value is equal to $\tau_{h\text{-Si}} = 4$ ns at 3.6 K according to Eqs. (24) and (28).

Since it is known that the cross-section is around $\sigma_{e-A} = 2 \times 10^{-16}$ cm^2 for the e-A transitions in the GaAs [34], one may suppose that the cross-section for the free hole to the donor transition in GaAs (σ_{h-D}) may be in the order of 2.4×10^{-14} cm^2.

Conclusions

The dynamics of the impurity-related optical transitions in 20 nm wide silicon and beryllium δ-doped GaAs/AlAs multiple QW's with various doping levels is investigated near liquid helium temperatures ($T = 3.6$ K) within picosecond scale excitation. The radiative lifetimes of the free electron-neutral acceptor and the free hole-neutral donor are experimentally studied and determined. The capture cross-sections derived from recombination lifetimes have been found to be $\sigma_{e\text{-Be}} = 4 \times 10^{-10}$ cm and $\sigma_{h\text{-Si}} = 2.2 \times 10^{-8}$ cm, respectively, in 20 nm wide beryllium and silicon δ-doped GaAs/AlAs multiple QW's. These results have been interpreted by adapting the theory of the fractional-dimensional space approach. The measured recombination lifetime for the Be δ-doped $N_{\mathrm{Be}} = 5.0 \times 10^{10}$ cm^{-2} MQWs corresponds to $\tau_{e\text{-Be}} = 11$ ns and is calculated to $\tau_{e\text{-Be}} = 7.3$ ns at 3.6 K. Consequently, for the Si δ-doped $N_{\mathrm{Si}} = 4.0 \times 10^9$ cm^{-2} MQWs, the measured recombination lifetime was found to be equal to $\tau_{h\text{-Si}} = 6$ ns, whereas the calculated value is equal to $\tau_{h\text{-Si}} = 4$ ns at 3.6 K. Hence a good agreement between the theory and the experiment was achieved.

References

[1] S.D. Gunapala, D.R. Rhiger, and C. Jagadish, *Advances in Infrared Photodetectors*, Semiconductors and Semimetals, Vol. 84 (Academic Press, San Diego, 2011).

[2] B.F. Levine, Quantum-well infrared photodetectors, J. Appl. Phys. **74**(8), R1–81 (1993).

[3] X.G. Guo, Z.Y. Tan, J.C. Cao, and H.C. Liu, Many-body effects on terahertz quantum well detectors, Appl. Phys. Lett. **94**(20), 201101 (2009).

[4] D. Seliuta, J. Kavaliauskas, B. Čechavičius, S. Balakauskas, G. Valušis, B. Sherliker, M.P. Halsall, P. Harrison, M. Lachab, S.P. Khanna, and E.H. Linfield, Impurity bound-to-unbound terahertz sensors based on beryllium and silicon δ-doped GaAs/AlAs multiple quantum wells, Appl. Phys. Lett. **92**(5), 053503 (2008).

[5] J. Kundrotas, A. Čerškus, S. Ašmontas, G. Valušis, B. Sherliker, M.P. Halsall, M.J. Steer, E. Johannessen, and P. Harrison, Excitonic and impurity-related optical transitions in Be δ-doped GaAs/AlAs

multiple quantum wells: Fractional-dimensional space approach, Phys. Rev. B **72**(23), 235322 (2005).

[6] J. Kundrotas, A. Čerškus, G. Valušis, A. Johannessen, E. Johannessen, P. Harrison, and E.H. Linfield, Impurity-related photoluminescence line shape asymmetry in GaAs/AlAs multiple quantum wells: Fractional-dimensional space approach, J. Appl. Phys. **107**(9), 093109 (2010).

[7] J. Feldmann, G. Peter, E.O. Göbel, P. Dawson, K. Moore, C. Foxon, and R.J. Elliott, Linewidth dependence of radiative exciton lifetimes in quantum wells, Phys. Rev. Lett. **59**(20), 2337–2340 (1987).

[8] M. Gurioli, A. Vinattieri, M. Colocci, C. Deparis, J. Massies, G. Neu, A. Bosacchi, and S. Franchi, Temperature dependence of the radiative and nonradiative recombination time in GaAs/$Al_xGa_{1-x}As$ quantum-well structures, Phys. Rev. B **44**(7), 3115–3124 (1991).

[9] J.P. Bergman, P.O. Holtz, B. Monemar, M. Sundaram, J.L. Merz, and A.C. Gossard, Decay measurements of free- and bound-exciton recombination in doped GaAs/$Al_xGa_{1-x}As$ quantum wells, Phys. Rev. B **43**(6), 4765–4770 (1991).

[10] J. Martinez-Pastor, A. Vinattieri, L. Carraresi, M. Colocci, Ph. Roussignol, and G. Weimann, Temperature dependence of exciton lifetimes in GaAs/$Al_xGa_{1-x}As$ single quantum well, Phys. Rev. B **47**(16), 10456–10460 (1993).

[11] *PMS-300, PMS-400 and PMS-400A 800 MHz Gated Photon Counters/Multiscalers* (Becker & Hickl GmbH, Berlin, 2004).

[12] W. Becker, *The bh TCSPC Handbook*, 4th ed. (Becker & Hickl GmbH, Berlin, 2010).

[13] J. Kundrotas, A. Čerškus, G. Valušis, L.H. Li, E.H. Linfield, A. Johannessen, and E. Johannessen, Light emission lifetimes in *p*-type *δ*-doped GaAs/AlAs multiple quantum wells near the Mott transition, J. Appl. Phys. **112**(4), 043105 (2012).

[14] K. Muraki, Y. Takahashi, A. Fujiwara, S. Fukatsu, and Y. Shiraki, Enhancement of free-to-bound transitions due to resonant electron capture in Be-doped AlGaAs/GaAs quantum wells, Solid State Electron. **37**(4–6), 1247–1250 (1994).

[15] A. Fujiwara, K. Muraki, S. Fukatsu, Y. Shiraki, and R. Ito, Enhancement of nonradiative recombination due to resonant electron capture in $Al_xGa_{1-x}As$/GaAs quantum-well structures, Phys. Rev. B **51**(20), 14324–14329 (1995).

[16] G.E. Stillman, C.M. Wolfe, and J.O. Dimmock, Magnetospectroscopy of shallow donors in GaAs, Solid State Commun. **7**, 921–925 (1969).

[17] J. Kundrotas, G. Valušis, A. Čėsna, A. Kundrotaitė, A. Dargys, A. Sužiedėlis, J. Gradauskas, S. Ašmontas, and K. Köhler, Excitonic photoluminescence quenching by impact ionization of excitons and donors in GaAs/$Al_{0.35}Ga_{0.65}As$ quantum wells with an in-plane electric field, Phys. Rev. B **62**(23), 15871–15878 (2000).

[18] J.M. Ballingall, B.J. Morris, D.J. Leopold, and D.L. Rode, Silicon autocompensation in GaAs grown by molecular-beam epitaxy, J. Appl. Phys. **59**, 3571–3573 (1986).

[19] S.S. Bose, B. Lee, M.H. Kim, G.E. Stillman, and W.I. Wang, Influence of the substrate orientation on Si incorporation in molecular-beam epitaxial GaAs, J. Appl. Phys. **63**(3), 743–748 (1988).

[20] K. Hess, D. Bimberg, N.O. Lipari, J.U. Fischbach, and M. Altarelli, Band parameter determination of III–V compounds from high-field magnetoreflectance of excitons, in: *Proceedings of the 13th International Conference on the Physics of Semiconductors* (Tipografia Marves, Rome, 1976) pp. 142–145.

[21] F.H. Stillinger, Axiomatic basis for spaces with noninteger dimension, J. Math. Phys. **18**(6), 1224–1234 (1977).

[22] J. Kundrotas, A. Čerškus, S. Ašmontas, G. Valušis, M.P. Halsall, E. Johannessen, and P. Harrison, Impurity-induced Huang–Rhys factor in beryllium *δ*-doped GaAs/AlAs multiple quantum wells: fractional-dimensional space approach, Semicond. Sci. Technol. **22**(9), 1–7 (2007).

[23] X.F. Xe, Anisotropy and isotropy: A model of fraction-dimensional space, Solid State Commun. **75**(2), 111–114 (1990).

[24] X.F. Xe, Fractional dimensionality and fractional derivative spectra of interband optical transitions, Phys. Rev. B **42**(18), 11751–11756 (1990).

[25] X.F. Xe, Excitons in anisotropic solids: The model of fractional-dimensional space, Phys. Rev. B **43**(3), 2063–2069 (1991).

[26] W.P. Dumke, Optical transitions involving impurities in semiconductors, Phys. Rev. **132**(5), 1998–2002 (1963).

[27] H.B. Beeb and E.W. Williams, Photoluminescence I: Theory, in: *Semiconductors and Semimetals*, eds. R.K. Willardson and A.C. Beer, Vol. 8 (Academic Press, New York, 1972) pp. 181–320.

[28] D.M. Eagles, Optical absorption and recombination radiation in semiconductors due to transitions between hydrogen-like acceptor impurity levels and the conduction band, J. Phys. Chem. Solids **16**(16), 76–83 (1960).

[29] C. Klingshirn, *Semiconductor Optics*, 2nd ed. (Springer, Berlin, 2005).

[30] P.K. Basu, *Theory of Optical Processes in Semiconductors: Bulk and Microstructures* (Clarendon Press, Oxford, 1997).

[31] J.H. Davies, *The Physics of Low-Dimensional Semiconductors: An Introduction* (Cambridge University Press, New York, 1997).

[32] G. Bastard, *Wave Mechanics Applied to Semiconductor Heterostructures* (Les Edition de Physique, Les Ulis Cedex, 1990).

[33] J. Singh, *Electronic and Optoelectronic Properties of Semiconductor Structures* (Cambridge University Press, New York, 2003).

[34] D. Bimberg, H. Münzel, A. Steckenborn, and J. Christen, Kinetics of relaxation and recombination of nonequilibrium carriers in GaAs: Carrier capture by impurities, Phys. Rev. B **31**(12), 7788–7799 (1985).

KRŪVININKŲ OPTINIŲ ŠUOLIŲ Į NEUTRALIĄSIAS PRIEMAIŠAS DINAMIKA Be IR Si δ-LEGIRUOTOSE GaAs/AlAs KARTOTINĖSE KVANTINĖSE DUOBĖSE: TRUPMENINIO MATUMO ERDVĖS ARTĖJIMAS

J. Kundrotas [a], A. Čerškus [a], G. Valušis [a], E.H. Linfield [b], E. Johannessen [c], A. Johannessen [c]

[a] *Fizinių ir technologijos mokslų centro Puslaidininkių fizikos institutas, Vilnius, Lietuva*

[b] *Lidso universitetas, Lidsas, Jungtinė Karalystė*

[c] *Buskerudo ir Vestfoldo universitetinis koledžas, Borre, Norvegija*

Santrauka

Kvantinių duobių elektrinės ir optinės savybės priklauso ne tik nuo jų matmenų, bet ir nuo legiruojančių priemaišų tipo bei tankio. Puslaidininkiuose seklios priemaišos turi apibrėžtas aktyvacijos energijas bei energinius lygmenų spektrus. Kvantinėse duobėse priemaišų energinį spektrą galima mainyti keičiant kvantinės duobės plotį. Atsiranda galimybė gauti įvairias priemaišų aktyvacijos energijas, kurios yra svarbios kuriant terahercinio dažnio emiterius ar jutiklius.

Laisvųjų krūvininkų rekombinacinių vyksmų dinaminės savybės yra svarbios aprašant optines kvantinių duobių savybes. Vieni iš svarbiausių parametrų yra laisvųjų krūvininkų pagavimo skerspjūviai neutraliomis priemaišomis. Iki šiol šie skerspjūviai donorinėms ir akceptorinėms priemaišoms kvantinėse duobėse nėra nustatyti.

Šiame darbe tirtos kartotinės kvantinės duobės buvo užaugintos molekulinių pluoštelių epitaksijos būdu ant izoliacinių GaAs padėklų. Kvantinės GaAs 20 nm pločio duobės atskirtos 5 nm pločio AlAs barjerais. Į kiekvienos kvantinės duobės vidurį įterptas silicio (Si) donorinių arba berilio (Be) akceptorinių priemaišų δ sluoksnis.

Dinaminiai vyksmai tirti esant žemai kvantinių duobių gardelės temperatūrai T = 3,6 K. Fotoliuminescencijos žadinimui naudojome diodu kaupinamą Nd:LSB kietojo kūno pikosekundinį lazerį. Dinaminiai fotoliuminescencijos vyksmai buvo tiriami pasitelkus bėgant laikui koreliuotų pavienių fotonų skaičiavimo metodiką (TCSPC). Teoriškai nagrinėjant pagavimo skerspjūvius naudojome trupmeninio matumo erdvės modelį. Išmatuotos spinduliuotės gyvavimo trukmės rekombinuojant elektronams su neutraliaisiais akceptoriais yra $\tau_{e\text{-Be}} = 11$ ns, kai $N_{\text{Be}} = 5 \cdot 10^{10}$ cm^{-2}; rekombinuojant skylėms su neutraliaisiais donorais – $\tau_{h\text{-Si}} = 6$ ns, kai $N_{\text{Si}} = 4 \cdot 10^{9}$ cm^{-2}. Iš eksperimentiškai išmatuotų gyvavimo trukmių nustatytas elektronų pagavimo skerspjūvis neutraliaisiais Be akceptoriais lygus $\sigma_{e\text{-Be}} = 4 \cdot 10^{-10}$ cm bei skylių pagavimo skerspjūvis neutraliaisiais Si donorais – $\sigma_{h\text{-Si}} = 2{,}2 \cdot 10^{-8}$ cm. Eksperimentiškai nustatytas pagavimo skerspjūvių santykis lygus $\sigma_{h\text{-Si}}/\sigma_{e\text{-Be}} = 55$, o apskaičiuotas dvimačiams dariniams – $\sigma_{h\text{-}D}/\sigma_{e\text{-}A} = 64$. Gautas geras sutapimas tarp eksperimentinių ir teorinių rezultatų.